

DLD Pillar Shape Design for Efficient Separation of Spherical and Non-spherical Bioparticles

Shashi Ranjan, Kerwin Kwek Zeming, Roland Jureen, Dale Fisher, Yong Zhang

Section-1: Supplementary data

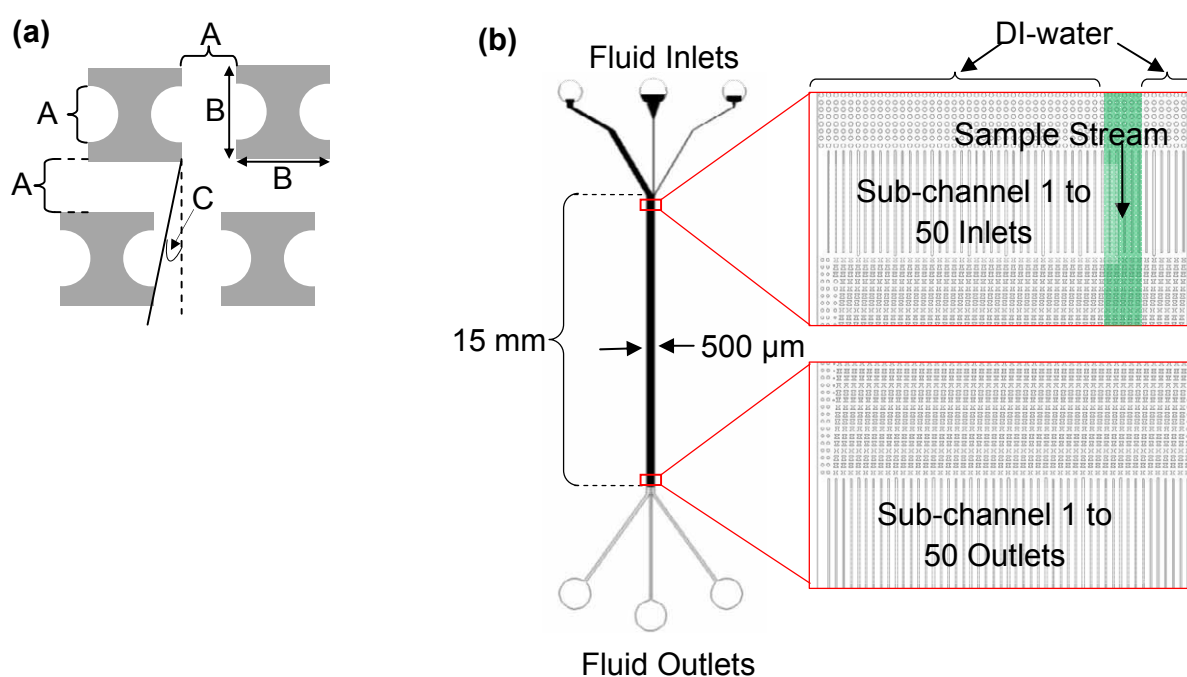


Figure-S1: Schematics for bacterial separation by I-shaped pillar array: (a) Dimensions of I-shaped pillars and DLD array components, where $A=4 \mu\text{m}$, $B=6 \mu\text{m}$ and $C=1.6^\circ$. (b) The layout of the microfluidic device containing I-shaped pillar array.

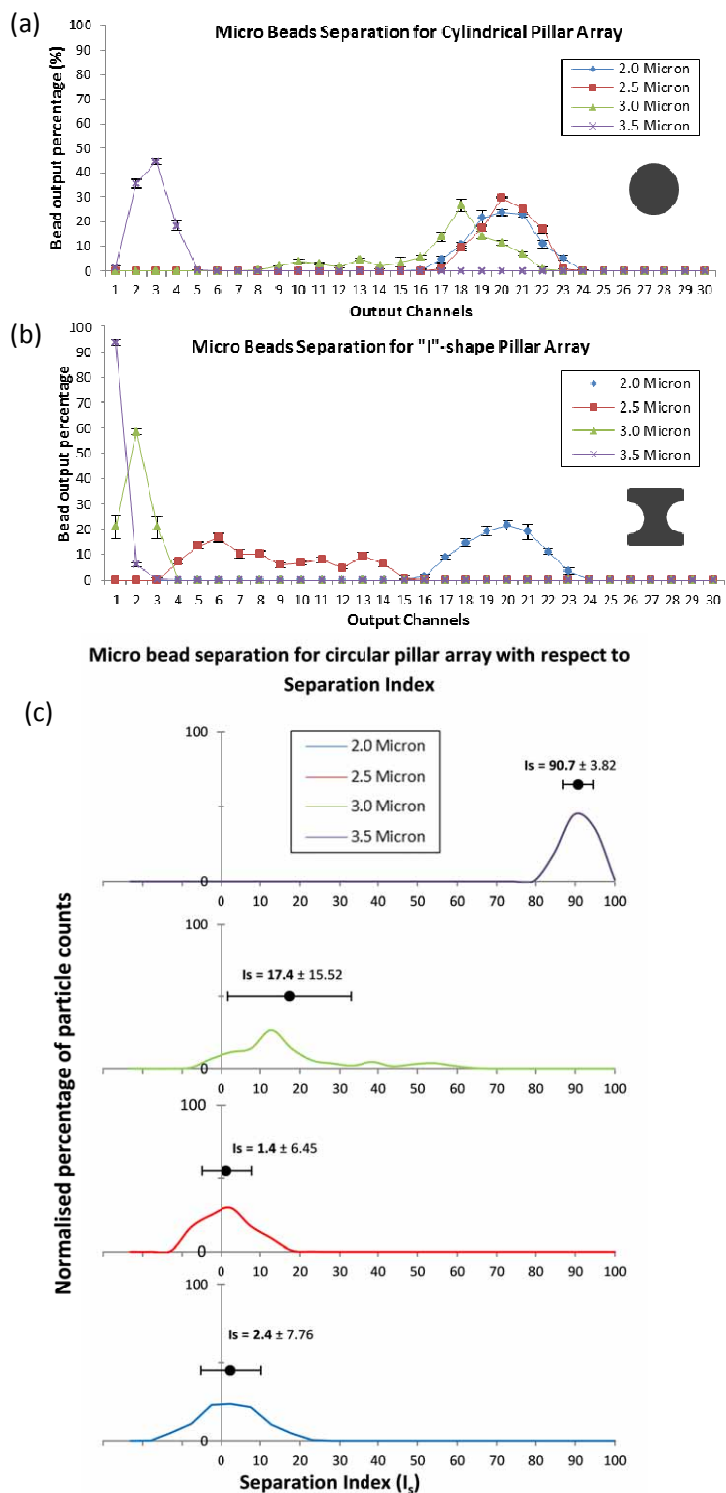


Figure S2. Conversion of bead separation data to Separation Index. Extracted graph from previous work showing separation of beads in circular (a) and I-shape pillar (b) array.¹ (c) is the corresponding conversion to the separation index (I_s).

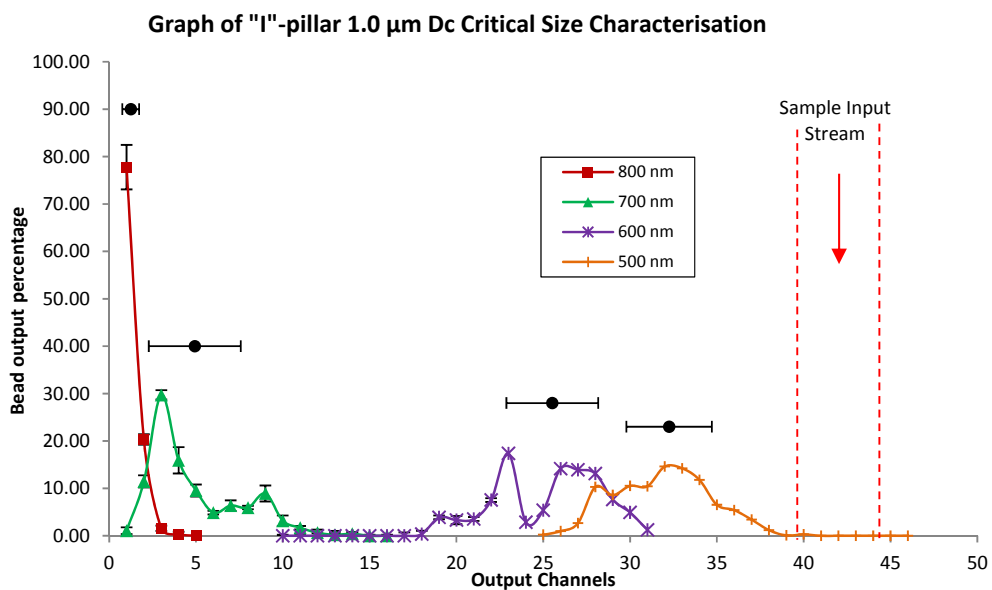


Figure S3. I-shape pillar bead based characterization. Determination of critical diameter of the I-shape device using beads of different sizes: the figure shows the output distribution of beads of different sizes flowed in the channels. The horizontal error bar represents the average distribution of the beads in the different channels. From this graph the critical diameter is estimated to be about 700nm.

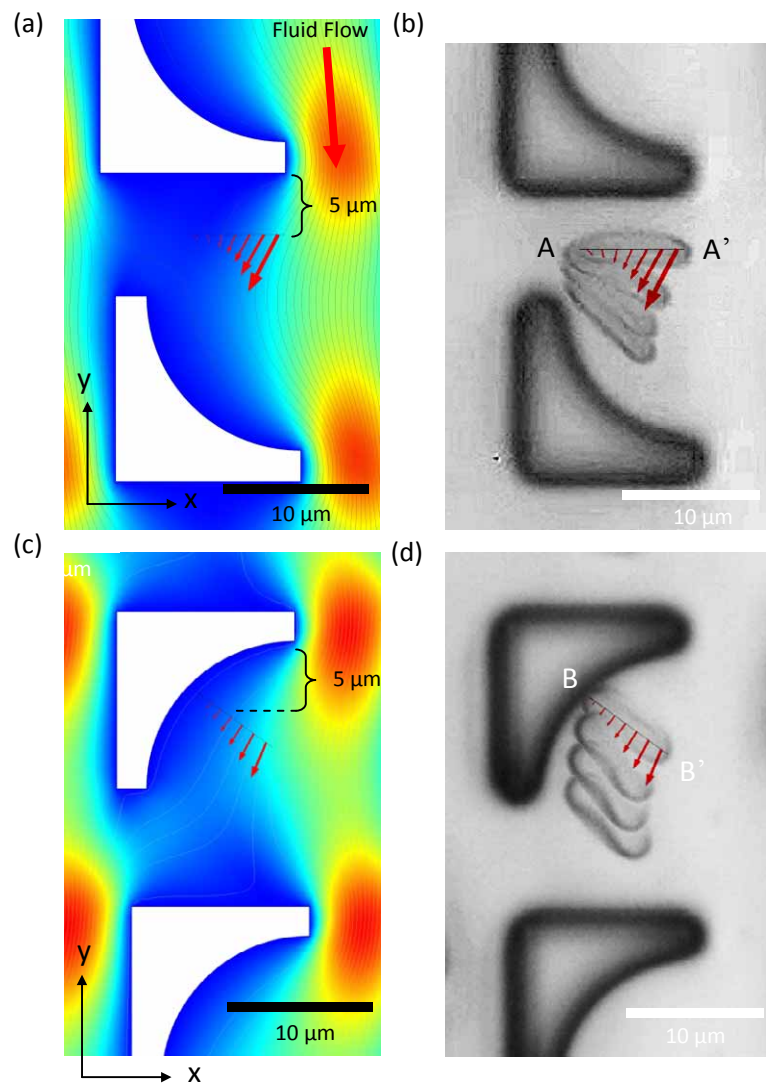


Figure S4: Computational analysis of fluid flux vector superimposed on RBC position for L-shape and inverted L-shaped pillars. (a) and (c) shows the COMSOL computational modeling with fluid flux represented in red arrows at the respective locations of RBC center positioned 5 μm after interacting with a pillar. (b) and (d) shows the respective experimental RBC position in the fluidic device with the same super imposed fluid flux vector.

Section-2: Materials and Methods

Detailed materials and methods are provided in this section.

Device Design and Fabrication: Two set of devices were used for this study. The first set of devices were used for the study of the separation of spherical and non-spherical particles using different pillar designs. The second set of the device was used for bacterial separation study. The layouts of the devices were designed using software AutoCAD and were printed as chrome-quartz photomask. The first set of devices consisted of three input streams of two buffer stream sandwiching the sample stream. Negative pressure was employed from the output of the device. The use of negative pressure enabled more control and consistency on the input stream position and width of the channel. Reservoirs of fluids were loaded at the input regions. The gradient of the DLD array was fixed at 1/20 and output channels were sub-divided into 26 channels. This subdivision enabled greater accuracy in characterization. Due to the input sheath stream, sub-channels 1 to 5 only contained the buffer stream. A simple size exclusion filter was designed into the sample input region to filter away bigger unknown particles or dust. The input stream remains from sub-channel 5 to 10.

The bacterial separation device comprised of three main inlets and three outlets. The middle inlet was designed for the introduction of sample into the device while the other two inlets were designed for the introduction of DI-water. The main separation channel was about 15 mm long and 500 μm wide. It consisted of 50 sub-channels at the inlet and at the outlet (Fig.S1b). The main channel consisted of the I-shaped pillar array with DLD dimensions of 4 μm of gap-size, 1.6° of pillar shift gradient and 6 μm of maximum pillar length (Fig.1a). The critical diameter of the circle pillar array was calculated by the formula derived by Davis *et al.*² as given below:

$$D_c = 1.4gN^{-0.48}$$

Where D_c = Critical diameter, g = gap size between pillars, N = Number of rows per shift in columns (i.e. $\tan^{-1}\frac{1}{N}$ = Gradient of pillar array)

Devices were fabricated on silicon wafers using standard photolithography and dry etching techniques under a clean-room facility located at the Institute of Materials Research and Technology. The device layout was transferred from the photomask to a thin layer of positive photoresist (AZ5214E, Microchem, MA) coated on a silicon wafer (at 4000 rpm for 1 min and baked at 95°C for another 1 min) by using a standard photolithography equipment (Karl SUSS MA8 Mask-aligner). It was developed and hard baked at 125°C to obtain the required pattern. It was followed by deep reactive ion etching using Oxford 180 dry reactive ion etching machine to a depth of about 9 μm to obtain pillars. Photoresist pattern acted as the mask for dry etching. A total of about 15 cycles were used to obtain this depth. After dry etching, the photoresist was removed by washing it with acetone for 1 min and dipping it in AZ300T (Hoechst, NJ) photoresist stripper for 10 min at 80°C. It was finally rinsed with DI-water. A thin sheet of Polydimethylsiloxane (Dow Chemicals, MI) with holes punched for inlets and outlets was prepared by adding base and curing solution in 10:1 ratio, followed by degassing and curing at 70°C for 60 min. It was bonded to the silicon microfluidic channels by using oxygen plasma with manual alignment.

Sample and reagent preparations:

All microfluidic devices were treated with (Tridecafluoro-1,1,2,2-tetrahydrooctyl)-1-trichlorosilane in a vacuum chamber for 30 min followed by Iso-propanol (IPA) and DI water wash for 30 mins; 1% (w/v) pluronic F127 (Sigma, Singapore) was used for priming and surface

treatment and 1x PBS buffer for dilution of blood and cell buffer stream. To prime the device, 1% (w/v) pluronic solution was directly loaded into the device using negative pressure for 30 mins. This sufficiently coated the surface of the silicon wafer (reference on pluronic). The device was washed with DI for 15 mins and the device is ready to be used.

Spherical micro-sphere: NIST Polystyrene micro-spheres (Bangs Laboratories, IN, United States) were used for characterization of device and to test effects of spherical particle separation within various pillars. For micro-sphere based separation, the micro-spheres were loaded into 1% (w/v) pluronic solution to prevent any form of unspecific binding. The fluid sheath flows were also 1% (w/v) pluronic solutions. The beads used were NIST beads of sizes 2.58 μm , 3.0 μm and 3.58 μm .

Red Blood Cells: The red blood cells were directly diluted in 1x PBS solution in a ratio of 1:20 (blood:PBS). Direct dilution resulted maintains the balance of ionic concentration needed for the bi-concave shape and enable clearer observation of each red blood cell. Each sample was not used for more than 24 hours and was kept in the 4 degrees Celsius fridge to prevent degradation of sample.

Bacterial sample preparation: HST08 strain of E. coli competent cells were purchased from Clontech (Singapore) and were transformed with pZsGreen vector also obtained from the same company. The vector contained a gene for conferring ampicillin resistance to E. coli was introduced into the E. coli by using heatshock protocols. It was cultured in LB broth solution containing 50 $\mu\text{g/ml}$ of ampicillin for about 20 hrs. Other bacteria were obtained from the Microbiology Laboratory at the National University Hospital, Singapore. These samples were obtained in broth solution and were fixed by using an equal volume of bacterial solution in broth

and the fixative solution (4% Glutaraldehyde (GA) + 4% Paraformaldehyde (PF) in PBS) at 4°C overnight. The fixed bacteria were washed and re-suspended in DI-water. These cells were labeled by using incubating fixed bacteria with Syto13 dye (Invitrogen, Singapore) for 30 min followed by washing. The final concentration of bacteria used for experiments was about 10^7 bacteria/ml.

Experimental setup and data analysis:

All experiments on bead and cells would flow into the device for a minute before starting the experiment. This is to ensure the fluid stream are stable first before capturing of video data using a Phantom M310 at varying frame rates from 100 fps to 1500 fps depending on flow-rates and magnification. The bead-based characterization samples and RBCs were sampled at 0.2 $\mu\text{l}/\text{min}$ while the bacterial samples were driven at a total flow rate 0.1 $\mu\text{l}/\text{min}$. The high speed video was eventually slowed to 25 fps to be analysed. COMSOL multiphysics 4.1 was used to model fluid dynamics of the various pillars.

Section-3: Study of bacterial adhesion to the device surfaces

The non-specific attachment of pathogens on different types of surfaces is well known^{3, 4}. This problem may result in significant loss of bacteria affecting experimental results. Although different surface treatment have been proposed in the literature, here the problem has been solved by applying surface coating of Pluronic F-127 over silane ((Tridecafluoro-1,1,2,2-tetrahydrooctyl)-1-trichlorosilane). Adsorption of Pluronic over hydrophobic surfaces (like the silanized surface) allow formation of brush-like confirmation of pluronic molecules⁵. Such confirmation prevents bacterial adhesion. A study was performed to obtain the correct percentage of Pluronic that can optimally prevent bacterial adhesion (Fig.S2). The result here

shows that combination of silane and Pluronic is much better compared to when they are used alone. From here, 1% pluronic was chosen for the rest of experiment as increased percentage caused frequent device failure due to resistance that they create to the fluid flow. Thus, the devices were treated with silane, followed by 1% pluronic, followed by through washing with DI-water before experiments were started.

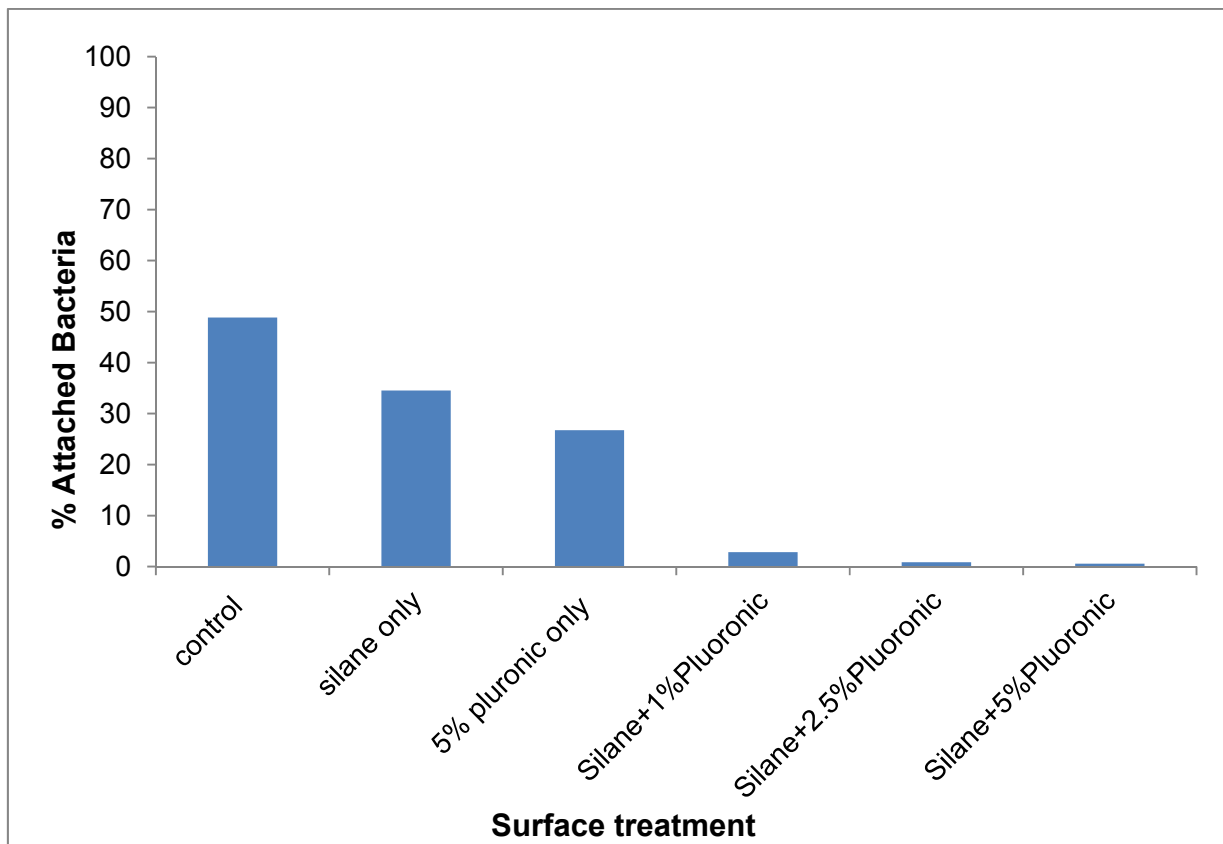


Figure-S4: The bacterial attachment to the surface of the DLD device in terms of percentage of bacteria attached on the device is presented. The plot here represents percent of bacteria that attached to the device surface out of total bacteria used for the experiment.

Movie Legends:

Movie-1: Flow of spherical micro-spheres in the I-shaped pillar array

Movie-2: Movements of RBCs through the I-shaped pillar array

Movie-3: Movements of RBCs through the L-shaped pillar array

Movie-4: Movements of RBCs through the Inverted L-shaped pillar array

Movie-5: Movements of rod shaped bacteria through the I-shaped pillar array

1. **K. K. Zeming, S. Ranjan and Y. Zhang, *Nat Commun*, 2013, 4, 1625.**
2. **P. M. Korczyk, L. Derzsi, S. Jakiela and P. Garstecki, *Lab on a chip*, 2013.**
3. **H. N. Abdelhamid and H.-F. Wu, *Journal of Materials Chemistry B*, 2013, 1, 3950-3961.**
4. **A. F. Coskun, R. Nagi, K. Sadeghi, S. Phillips and A. Ozcan, *Lab on a chip*, 2013.**
5. **A. F. Sauer-Budge, P. Mirer, A. Chatterjee, C. M. Klapperich, D. Chargin and A. Sharon, *Lab on a chip*, 2009, 9, 2803-2810.**